

# ***Radiation Effects in Nuclear Ceramics for the Immobilization of Radioactive Waste***

*A THESIS SUBMITTED*  
*TO*  
**THE MAHARAJA SAYAJIRAO UNIVERSITY OF BARODA**



*FOR THE DEGREE OF*  
**DOCTOR OF PHILOSOPHY**

*IN*  
**PHYSICS**

*BY*  
**Asha**

*UNDER THE GUIDANCE OF*  
**Prof. N. L. SINGH**

**DEPARTMENT OF PHYSICS,  
FACULTY OF SCIENCE,  
THE MAHARAJA SAYAJIRAO UNIVERSITY OF BARODA,  
VADODARA-390002, GUJARAT, INDIA  
NOVEMBER-2021**

## Table of Contents

List of Figures.....	i
List of tables.....	iv
1. Introduction.....	2
1.1 Background.....	2
1.2 Types of Nuclear wastes.....	3
1.3 Crystalline ceramic host matrices for nuclear waste.....	4
1.4 Pyrochlore oxides.....	4
1.4.1 Structure of the pyrochlore oxides.....	5
1.4.2 $A_2^{3+}B_2^{4+}O_7$ pyrochlore oxides.....	7
1.5 Motivation.....	14
1.6 Scope and Goals of Thesis.....	15
1.7 Thesis objectives.....	15
1.8 Structure of the Thesis.....	15
References.....	16
2. Synthesis method and experimental techniques.....	26
2.1 Introduction.....	26
2.2 Preparation of $La_2Zr_2O_7$ and $Gd_2Zr_2O_7$ matrices.....	26
2.2.1 Materials.....	26
2.2.2 Solid-state method.....	27
2.2.3 Synthesis of $La_2Zr_2O_7$ and $Gd_2Zr_2O_7$ .....	27
2.3 Irradiation Experiments.....	28
2.4. Analytical characterization tools.....	31
2.4.1 X-ray diffraction (XRD).....	31
2.4.2 Grazing Incidence X-ray Diffraction (GIXRD).....	33
2.4.3 Field Emission Scanning Electron Microscopy.....	34
2.4.4. Raman spectroscopy.....	35
2.4.5. High-resolution transmission electron microscopy (HR-TEM).....	37
References.....	40
3. Impact of annealing temperature on structural and microstructural properties of $La_2Zr_2O_7$ pyrochlore.....	43
3.1 Introduction.....	43
3.2 Results and Discussion.....	43

3.2.1 Structural analysis: XRD.....	43
3.2.1.1 Rietveld Refinement Analysis.....	45
3.2.2 FESEM Analysis.....	48
3.3 Conclusion.....	53
References.....	54
4. Structural response of $\text{La}_2\text{Zr}_2\text{O}_7$ pyrochlore upon irradiation with 1.0 MeV $\text{Xe}^{4+}$ ions.....	58
4.1 Introduction.....	58
4.2 Results and Discussion.....	59
4.2.1 FE-SEM study.....	59
4.2.2 SRIM simulation.....	60
4.2.3 GIXRD analysis.....	60
4.2.4 Rietveld analysis.....	65
4.2.5 Analysis of vibrational mode: Raman spectroscopy.....	66
4.2.6 HR-TEM analysis.....	69
4.3 Conclusion.....	70
References.....	71
5. Investigation of atomic order-disorder in the $\text{La}_2\text{Zr}_2\text{O}_7$ pyrochlore under low energy (500 keV, $\text{Kr}^{2+}$ ) ion irradiation.....	76
5.1 Introduction.....	76
5.2 Results and Discussion.....	76
5.2.1 FE-SEM analysis.....	76
5.2.2 GIXRD analysis.....	77
5.2.3 Rietveld refinement analysis.....	81
5.2.4 Raman analysis.....	84
5.3 Conclusion.....	88
References.....	89
6. Role of structural ordering on the radiation resistance response of $\text{Gd}_2\text{Zr}_2\text{O}_7$ pyrochlore.....	95
6. 1 Introduction.....	95
6.2 Results and Discussion.....	96
6.2.1 Structural and microstructural properties of GZO: Impact of sintering temperature....	96
6.2.2 Impact of irradiation on sintered GZO: Radiation tolerance study.....	105
6.3 Conclusion.....	111

References.....	112
7. Structural modifications of $\text{Gd}_2\text{Zr}_2\text{O}_7$ pyrochlore induced by swift heavy ions for nuclear waste immobilization.....	117
7.1	
Introduction.....	117
7.2. Results and Discussion.....	118
7.2.1 Phase and microstructure analysis of pristine GZO.....	118
7.2.1 Radiation damage upon ion irradiation of 100 MeV $\text{I}^{7+}$ ions.....	120
7.3 Conclusion.....	127
References.....	128
8. Summary and Conclusions.....	133
8.1 Summary and Conclusions.....	133
8.2 Future Perspectives.....	138
9. List of Publications.....	139

## Contents of Thesis Summary

1.1 Introduction.....	7
1. 2 Experimental Method.....	10
1.2.1 Preparation and ion irradiation experiments .....	10
1.2.2 Characterizations.....	11
1.3 Key Finding .....	11
1.3.1 Modification of structural and microstructural properties of $\text{La}_2\text{Zr}_2\text{O}_7$ by annealing temperature and time .....	11
1.3.2 Ion irradiation (1.00 MeV $\text{Xe}^{4+}$ and 500 keV $\text{Kr}^{2+}$ ) induced structural modifications in $\text{La}_2\text{Zr}_2\text{O}_7$ .....	12
1.3.3 Radiation tolerance of $\text{Gd}_2\text{Zr}_2\text{O}_7$ upon irradiation swift heavy ion irradiation: a suitable matrix for immobilization of nuclear waste .....	15
1.4 Conclusions.....	16
References.....	20

## Thesis Summary

Continuous increase in population and thereby increase in the demand for energy from all over the world is attracting the scientific community towards the search for a clean and reliable energy source. Nuclear energy can be a great solution as the proponents mark it as a clean, reliable, and sustainable energy source with reduced carbon emissions; and hence it can make a significant contribution to global energy needs [1]. Nuclear power generation is one of the most important and useful applications of nuclear reactors as it can moderately substitute fossil fuels. But, “If the spread of nuclear energy cannot be decoupled from the spread of nuclear weapons, it should be phased out” [1]. However, keeping the positive side on sight; researchers are trying to solve the concerns related to nuclear energy production. One of them is radioactive waste; by-products of the nuclear fuel cycle (NFC). The NFC operations involve the operation of the reactor, recycling of spent fuel, and fabrication of fuel, and producing nuclear waste which includes high, intermediate, and low-level radioactive waste (HLW, ILW, and LLW). Not only NFCs but also the nuclear power generation and other nuclear-related applications, for example, fusion and fission industry, defence programs, research, and agriculture produce nuclear radioactive waste as a by-product. To assure the tenable application of nuclear energy, it is pivotal to manage nuclear waste, especially HLW, securely and cogently. The HLW should be immobilized to ensure its safety for storage, transportation, and final repository disposal [2–4]. The challenges that are considered for selecting a waste form include, but are not limited to (i) ability to upload large radioactive waste, (ii) easy production of the system, (iii) high radiation stability under environmental conditions, (iv) possible upload of the mixture of radioactive nuclides and other pollutant species resulting in minimal secondary phases creation, (v) must be agreeable with ‘near field environment’ of the waste geological repository, *etc.* [4].

Ceramic materials based on different compositions have been examined against the immobilization of radionuclide waste and actinides transmutations [5]. Based on the requirements, there are several forms of crystalline ceramics phase which have been utilized for radioactive waste immobilization [5]. Among the ceramic crystalline compounds, the pyrochlore oxides have been considered a promising candidate for the immobilization of radioactive nuclear waste [5].

In the present investigation, we have prepared a series of zirconate pyrochlore oxides, namely,  $\text{La}_2\text{Zr}_2\text{O}_7$  and  $\text{Gd}_2\text{Zr}_2\text{O}_7$  via a standard solid-state method. Firstly, the  $\text{La}_2\text{Zr}_2\text{O}_7$  samples were annealed at three different temperatures (1200, 1300, and 1500°C) and time (24, 48, and 96 h), to investigate the impact of annealing temperature and time on the structural and

microstructural properties. Secondly, the  $\text{La}_2\text{Zr}_2\text{O}_7$  samples were subjected to lighter ion  $\text{Xe}^{4+}$  and  $\text{Kr}^{2+}$  irradiation at two different temperatures (88 K and 300 K), to explore and elucidate the light energy ions induced structural transformations as a function of irradiation temperature and ion fluence. Lastly, the  $\text{Gd}_2\text{Zr}_2\text{O}_7$  were subjected to swift heavy (100 MeV)  $\text{I}^{7+}$  ions irradiation to investigate the radiation tolerance as a function of different degrees of structural ordering and ion fluence for possible use in nuclear applications. The pristine and post irradiated  $\text{La}_2\text{Zr}_2\text{O}_7$  and  $\text{Gd}_2\text{Zr}_2\text{O}_7$  were analyzed by XRD, GIXRD, FE-SEM, Raman spectroscopy, and HR-TEM. Consequently, structural and microstructural properties of  $\text{La}_2\text{Zr}_2\text{O}_7$  and  $\text{Gd}_2\text{Zr}_2\text{O}_7$  systems as a function of annealing time, irradiation temperature, ion energy, and ion fluence were investigated. To achieve the objective of the present research work, the thesis is divided into eight chapters, and the content of each chapter is as follows. Chapter-1 includes a brief discussion of different types of radioactive waste and actinides and an overview of the challenges that should be considered for selecting waste forms. The distinctive crystalline ceramic host matrices are explored for radioactive waste immobilization. A comprehensive review on how external parameters, i.e., chemical substitution, annealing temperature, pressure, irradiation temperature, and ion energy modified the structural properties of pyrochlore oxides have also been discussed. The features of pyrochlore oxides that make them different from other ceramic oxides are also explained. Chapter-2 describes the synthesis method, irradiation process, and different characterization techniques used for analyzing the  $\text{La}_2\text{Zr}_2\text{O}_7$  and  $\text{Gd}_2\text{Zr}_2\text{O}_7$  samples. The evaluation of structural and microstructural properties of  $\text{La}_2\text{Zr}_2\text{O}_7$  with the enhancement of annealing temperature and time is discussed in chapter-3. The ion irradiation, 100 MeV  $\text{Xe}^{4+}$ , and 500 keV  $\text{Kr}^{2+}$ , induced structural modifications with the function of irradiation temperature (i.e., 88 K and 300 K) and ion fluence are discussed successively in chapter-4 and chapter-5. The radiation tolerance capability of  $\text{Gd}_2\text{Zr}_2\text{O}_7$  samples with the function of structural ordering and ion fluence for the possible applications in hostiles environments, i.e., the safe and effective management of high-level radioactive waste and actinides in discussed in chapter-6 and chapter-7. Chapter-8 delineates the impressive results upon irradiation of  $\text{Xe}^{4+}$  and  $\text{I}^{7+}$  ions with a brief outline of future perfectives.

## 1.1 Introduction

The main source of radioactive wastes is the nuclear fuel cycle (NFC) which includes high-level radioactive waste [1]. These radioactive wastes are classified into three broad categories according to their radioactive content. These are defined as namely: (1) very low-level wastes (less than 400kBq/t of  $\beta$  and  $\gamma$  activity and can be eliminated with domestic waste), (2) low-level wastes (less than 4GBq/t of  $\alpha$  or 12Bq/t of  $\beta$  and  $\gamma$  activity), (3) intermediate-level wastes (contains activities more than low-level wastes, no heating effect of radioactive decay), (4) high-level waste (it contains the radioactive decay that produces ample heat which necessitates special design, storage, transport and disposal of waste) [6]. Among all these wastes high-level radioactive wastes need a special design for storage and disposal. The HLW wastes are hazardous and therefore needs proper management for immobilization [3,6] Immobilisation of high-level radioactive wastes (HLWs) is achieved by incorporating the radioactive waste chemically into an appropriate matrix structure (typically glasses or ceramics) to make it immobile and thus it is not able to escape into the environment [4,6]. To obtain the immobilization of HLW wastes, crystalline ceramics are found dominant for the current stage of modern nuclear technology development. Several types of ceramics have been designed with desired structures [7]. The Classification of crystalline ceramic compounds as suitable waste forms for the radioactive waste is presented in Fig. 1. The intent of the ceramics evolution was to emerge a waste form that must have superior physical, chemical, mechanical and thermal durability as compared to glass [5].

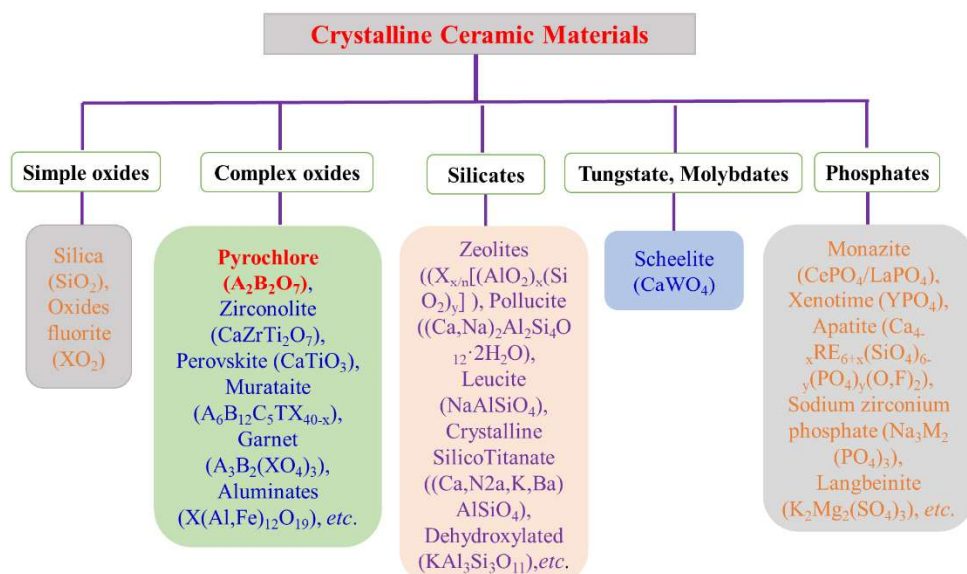
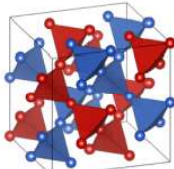


**Figure 1.** The Classification of crystalline ceramic compounds as suitable waste forms for radioactive waste.

Among the ceramic crystalline compounds, the pyrochlore matrices,  $A_2B_2O_7$ , provide an enormous band of structural and physical properties because of their numerous chemical compositions. In pyrochlore oxides family, particularly, the  $A_2^{3+}B_2^{4+}O_7$  compounds [Fig. 2] have caught huge attention in the radioactive waste management field because of the capability of incorporating actinides, i.e., Th, U, and Np, etc. [11].

H	$(\text{A}^{3+})_2(\text{B}^{4+})_2\text{O}_7$																He
Li	Be											B	C	N	O	F	Ne
Na	Mg											Al	Si	P	S	Cl	Ar
K	Ca	Sc	Ti	V	Cr	Mn	Fe	Co	Ni	Cu	Zn	Ga	Ge	As	Se	Br	Kr
Rb	Sr	Y	Zr	Nb	Mo	Tc	Ru	Rh	Pd	Ag	Cd	In	Sn	Sb	Te	I	Xe
Cs	Ba	La	Hf	Ta	W	Re	Os	Ir	Pt	Au	Hg	Tl	Pb	Bi	Po	At	Rn



Ce	Pr	Nd	Pm	Sm	Eu	Gd	Tb	Dy	Ho	Er	Tm	Yb	Lu
Th	Pa	U	Np	Pu	Am	Cm	Bk	Cf	Es	Fm	Md	No	Lr

**Figure 2.** The periodic table highlights elements with oxidation states, i.e.,  $3^+$  (red) and  $4^+$  (blue) which help to configuration the  $A_2^{3+}B_2^{4+}O_7$  pyrochlore phase.

The inevitable properties of the  $Ln_2Zr_2O_7$  pyrochlore oxides established them an appropriate aspirant for the important technological applications, for example, high-temperature superconductors, piezoelectricity, photoluminescence, immobilization of radioactive nuclear waste, catalysis, thermal barrier coatings, high-temperature solid oxide fuel cells, solid electrolytes, spin liquids, and so on [8–10]. It should be noted that the properties of the  $Ln_2Zr_2O_7$  compounds significantly depend on the structural ordering/ disordering and defects irradiation, temperature, or pressure. The mixed-phase  $La_2Zr_2O_7$  was found to have superior conductivity on account of lattice mismatch at the interface joining pyrochlore and defect fluorite phase. [11]. Previous studies suggest that  $La_2Zr_2O_7$  is admirable for immobilization of actinide (Pu can be fused at any of the cationic sites) wastes [12,13]. Ion-beam irradiations with energies varying from few keV to few MeV have been used to reproduce alpha-decay damage in a broad spectrum of pyrochlore compositions, particularly in  $A_2Zr_2O_7$  and  $A_2Ti_2O_7$  systems, in ion beam irradiation the incident ions produce interstitial atoms cascade and vacancies because of an incident ion and lattice structure's elastic collision. [14–16]. The smaller values of cationic radii ratio,  $r_A/r_B < 1.46$ , favored the formation of disordered fluorite phase [17]. With the cationic radii ratio of  $r_A/r_B = 1.46$ , the  $Gd_2Zr_2O_7$  lies on the boundary of the pyrochlore



and disordered fluorite phase. Therefore, the formation of disordered fluorite and/or pyrochlore phase  $\text{Gd}_2\text{Zr}_2\text{O}_7$  is uncomplicated by engineering the cationic disordering/ordering at certain temperatures [18]. Several SHI irradiations (energy range: MeV to GeV) researches were performed by Patel et al., Lang et al., and Sattonnay et al. and they reported that order-disorder transformation and amorphization induced by irradiation intensely rely on elemental composition [15,19–22].  $\text{Gd}_2\text{Zr}_{2-x}\text{Ti}_x\text{O}_7$  shows consistent enhancement in “resistance” to ion beam-induced amorphization with increased Zr content, and hence, the phase transformation is favored towards a disordered, defect-fluorite phase. After the maximal irradiation, the end member,  $\text{Gd}_2\text{Zr}_2\text{O}_7$ , which originally consists of a mixture of crystalline pyrochlore and defect-fluorite structure, is altered to the disordered, defect-fluorite structure with no signs of amorphization.

The development of radiation-resistant compounds for the effective management of radioactive wastes is of utmost importance. Based on the findings of the literature review, zirconate pyrochlores are cogitated to be significant host matrices for radioactive waste incorporation.

Processing and synthesis of ceramic and other materials should be designed with specific attention to controlling and changing the chemical and physical properties for promising use in modern era emerging applications. Therefore, there is a need for special attention to various synthesis tools for processing, synthesizing, and evaluating associated properties. Polycrystalline  $\text{La}_2\text{Zr}_2\text{O}_7$  and  $\text{Gd}_2\text{Zr}_2\text{O}_7$  ceramic compounds were prepared through a facile and economical synthesis approach, i.e., the standard solid-state method, which is one of the popular techniques for the preparation of ceramic materials [22,23]. To compute the effect of annealing temperature and time on  $\text{La}_2\text{Zr}_2\text{O}_7$  structural and microstructural properties,  $\text{La}_2\text{Zr}_2\text{O}_7$  was annealed at different temperatures and times. Ion irradiation induced structural modifications in the  $\text{La}_2\text{Zr}_2\text{O}_7$  matrices as a function of irradiation temperature, ion energy, and ion fluence were explored. Consequently, the structural changes of post irradiated matrices were evaluated using GIXRD, Raman spectroscopy, and HR-TEM. The impact of different degrees of structural defects on the radiation tolerance of  $\text{Gd}_2\text{Zr}_2\text{O}_7$  samples was investigated upon swift heavy ion irradiation (100 MeV  $\text{I}^{7+}$ ) and evaluated the capabilities of  $\text{Gd}_2\text{Zr}_2\text{O}_7$  samples for the possible applications in hostile environments such as radiation tolerant hosts for safe and effective management of radioactive nuclear wastes and surplus actinides.

## 1. 2 Experimental Method

### 1.2.1 Preparation and ion irradiation experiments

The solid-state process is a facile and economical synthesis method for the preparation of polycrystalline material.

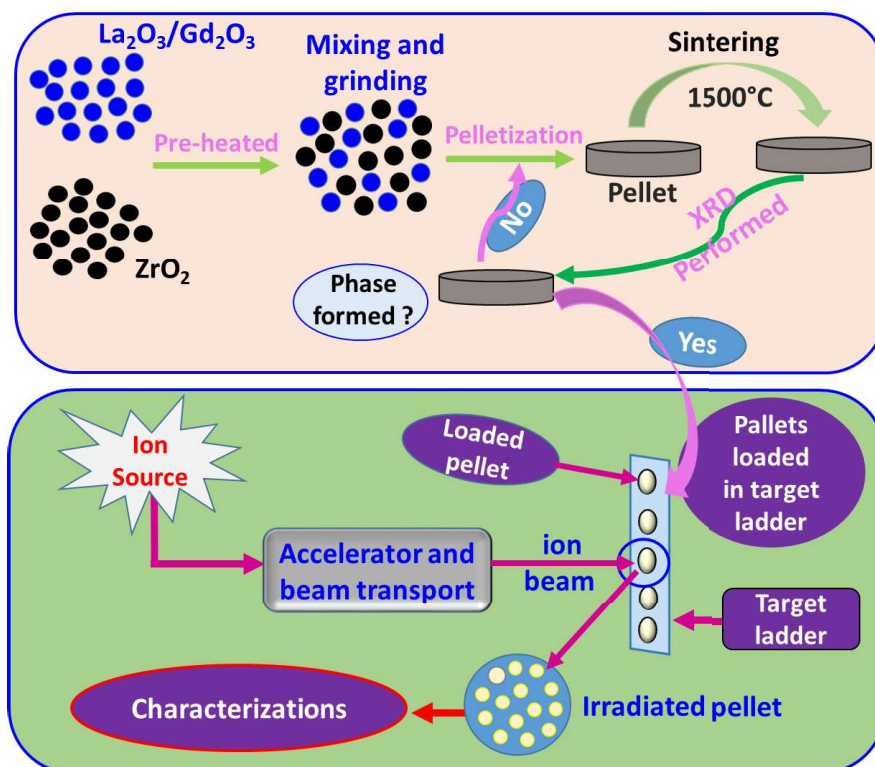


**Figure 3.** Schematic diagram of the synthesis and irradiation process of zirconate pyrochlore oxides.

This approach involves the mixing of reactants (in powder form) in stoichiometric ratio followed by several steps such as crushing, grinding, and milling till the formation of homogeneity. Thus, this technique includes mingling of powder precursors and step by step annealing for a longer duration at elevated temperature followed by intermittent grinding in between for sublime homogeneity. The schematic diagram of the preparation of zirconate pyrochlore oxides and irradiation process is illustrated in Fig. 3.

All irradiation experiments were conducted at Inter-University Accelerator Centre (IUAC), New Delhi. All the samples were loaded using tape on the target ladder to be placed inside the irradiation chamber. The irradiation ion beam was optimized for a  $1.0 \times 1.0 \text{ cm}^2$  scanning area in the X-Y plane. To ensure the desired beam size on the samples, the ion beam is first made to hit the quartz crystal and it is optimized before moving to target samples.

The parameters used for the ion irradiation experiment were calculated by employing the software called SRIM (Stopping and Range of Ions in Matter) 2013 [24]. The electronic energy

loss ( $S_e$ ) and nuclear energy loss ( $S_n$ ) and projectile range ( $R_p$ ) of  $\text{La}_2\text{Zr}_2\text{O}_7$  and  $\text{Gd}_2\text{Zr}_2\text{O}_7$  were simulated using SRIM 2013.

### 1.2.2 Characterizations

XRD and GIXRD measurements were performed using the Rigaku Smart Lab and Bruker D8 advance X-ray diffractometer ( $\lambda = 1.5406 \text{ \AA}$ ). The Debye Scherrer equation,  $D = K\lambda/\beta\cos\theta$  was utilized to deduce the average crystallite size. Moreover, the average crystallite size and lattice strain of zirconate pyrochlore oxides were determined using the expression,  $\beta = K\lambda/D\cos\theta + 4\varepsilon\tan\theta$ , which is called the Williamson-Hall equation. The W-H equation suggests that the peak broadening depends on the crystallite size and lattice strain. The Rietveld refinement of XRD patterns of  $\text{La}_2\text{Zr}_2\text{O}_7$  and  $\text{Gd}_2\text{Zr}_2\text{O}_7$  samples were refined using the Fullprof program. During the Rietveld refinement process, the Pseudo-Voigt function was used in the fitting of XRD patterns. The microstructure of  $\text{La}_2\text{Zr}_2\text{O}_7$  and  $\text{Gd}_2\text{Zr}_2\text{O}_7$  samples are investigated by field emission scanning electron microscopy (FESEM, Supra 55 Zeiss, UK). The Raman spectroscopy was performed to examine the disorder, lattice defects, and distortion in vibrational modes. Raman measurements of all samples presented here were performed using a micro-Raman model STR 500 with an excitation (wavelength of 785 nm) from an Nd-YAG laser source and argon laser source equipped Labram-HR 800 spectrometer (488 nm).

The deterioration of atomic ordering was investigated from high-resolution transmission electron microscopy. The JEOL 3010 high-resolution transmission electron microscope (HRTEM) is used to characterize the samples.

## 1.3 Key Finding

### 1.3.1 Modification of structural and microstructural properties of $\text{La}_2\text{Zr}_2\text{O}_7$ by annealing temperature and time

As we know, structural defects and microstructure of the constituting phase are major driving forces in all engineering materials to alter their chemical and physical properties. Therefore, to alter the structural and microstructural properties of  $\text{La}_2\text{Zr}_2\text{O}_7$  samples were annealed at different temperatures and times. Upon annealing at different temperatures and times, the  $\text{La}_2\text{Zr}_2\text{O}_7$  samples responded surprisingly, which was reflected in the associated structural and microstructural properties. XRD analysis revealed that the intensities of the reflection pattern enhance with the augmentation of annealing temperature and time owing to enhancement of crystallinity and grain size.

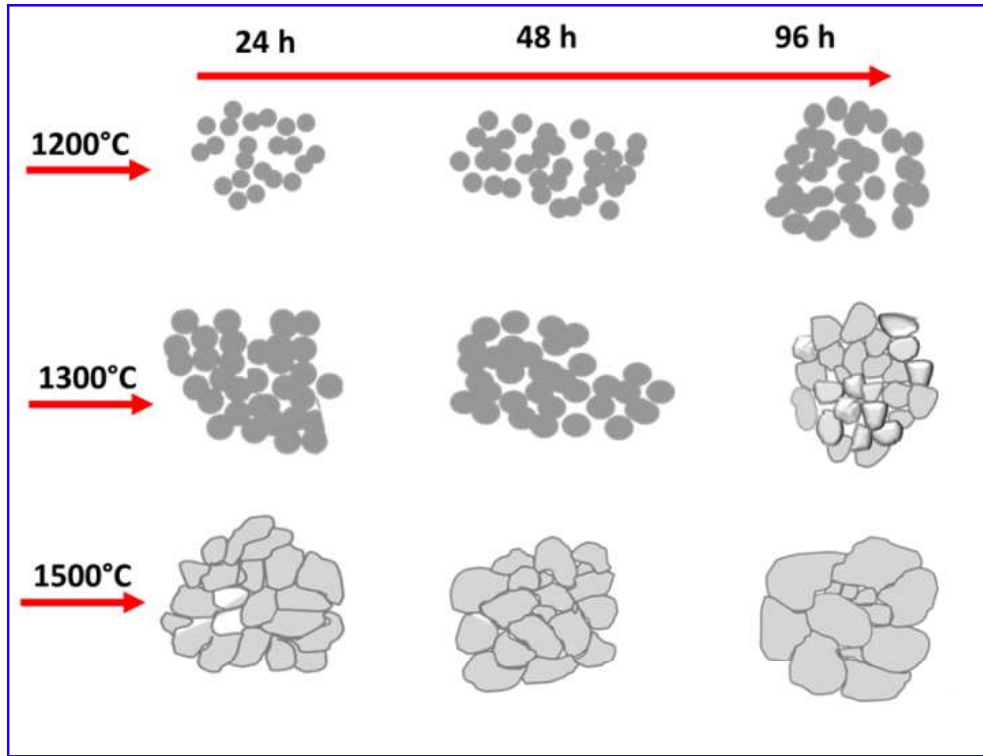


**Figure 4.** Evolution of grain growth of  $\text{La}_2\text{Zr}_2\text{O}_7$  samples as a function of annealing temperature and time.

Interestingly, the intensity of superstructure reflection, i.e., (111) enhanced with the extension of annealing duration and annealing temperature which specifies the pyrochlore phase ordering. Cation ordering quantified from the Rietveld refinement confirmed the pyrochlore phase ordering strongly supports the XRD analysis. FESEM revealed that the grain sizes enhanced and porosity decreased with the function of annealing temperature and time. The dependence of grain sizes on the annealing temperature and time is illustrated in Fig. 4. The curvature-driven grain growth is predominantly governed by the coarsening of remaining small grains and curvature-driven migration/diffusion of grain boundaries. An outcome of the investigation reveals that the annealing temperature and time are crucial parameters for designing the high dense and highly ordered materials for use in different fields.

### 1.3.2 Ion irradiation (1.00 MeV $\text{Xe}^{4+}$ and 500 keV $\text{Kr}^{2+}$ ) induced structural modifications in $\text{La}_2\text{Zr}_2\text{O}_7$

$\text{La}_2\text{Zr}_2\text{O}_7$  samples were irradiated using 1.00 MeV  $\text{Xe}^{4+}$  and 500 keV  $\text{Kr}^{2+}$  ions as a function of irradiation temperature (300 K and 88 K) and ion fluences, i.e.,  $1.0\text{E}13$ ,  $5.0\text{E}13$ , and  $1.0\text{E}14$  ion/ $\text{cm}^2$ . The dependence of structural modifications of  $\text{La}_2\text{Zr}_2\text{O}_7$  samples on irradiation temperature and ion fluence was investigated by GIXRD, Raman spectroscopy, and HR-TEM.

GIXRD studies were carried out to unveil the effects of ion irradiation on the structural response of  $\text{La}_2\text{Zr}_2\text{O}_7$  samples.

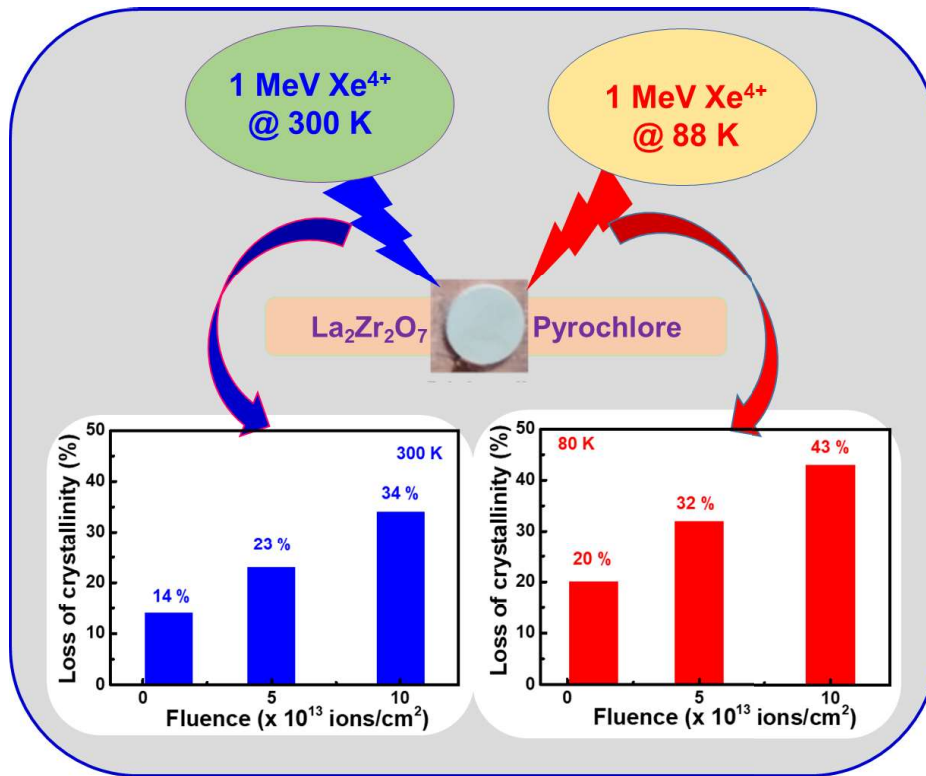


**Figure 5.** Dependence of loss of crystallinity (damage/amorphization) on irradiation temperature and ion fluence.

SRIM results exhibit that nuclear energy loss predominates in both irradiation studies. The reduction in the intensity of reflections is observed at both temperatures as a function of ion fluence upon irradiation of 1.0 MeV  $\text{Xe}^{4+}$  ions. The diminution of reflections intensity specifies the degradation of the crystallinity of  $\text{La}_2\text{Zr}_2\text{O}_7$  samples. The relatively widened and weakened reflections of  $\text{La}_2\text{Zr}_2\text{O}_7$  samples at  $\sim 88$  K indicate that the degradation of crystallinity is quite higher at  $\sim 88$  K than 300K.

Here, we wish to stress that upon ion irradiation of 1.0 MeV  $\text{Xe}^{4+}$  ions, the presence of superstructure reflections suggests that the  $\text{La}_2\text{Zr}_2\text{O}_7$  samples preserved the pyrochlore phase structure at both the temperatures, i.e., no signature of amorphization is observed. The irradiation-induced damage/amorphization (loss of crystallinity) in the  $\text{La}_2\text{Zr}_2\text{O}_7$  samples was determined by the relative variation in the full-width half maxima and observed that the deterioration of crystallinity is significantly prominent at 88 K due to the immobile nature of irradiation-induced defects.

The irradiation-induced damage/amorphization (loss of crystallinity) quantified from GIXRD and Raman spectroscopy analysis is illustrated in Fig. 5. The Raman spectroscopy analysis

revealed that the vibrational modes of post irradiated  $\text{La}_2\text{Zr}_2\text{O}_7$  samples are weakened and broadened with the increment of fluence at  $\sim 88$  K and 300 K. The weakened and broadened vibrational modes of  $\text{La}_2\text{Zr}_2\text{O}_7$  samples indicates that the vibrational modes deteriorated with the function of ion fluence. The damage/amorphization quantified from the Raman spectroscopy results strengthen the GIXRD analysis.

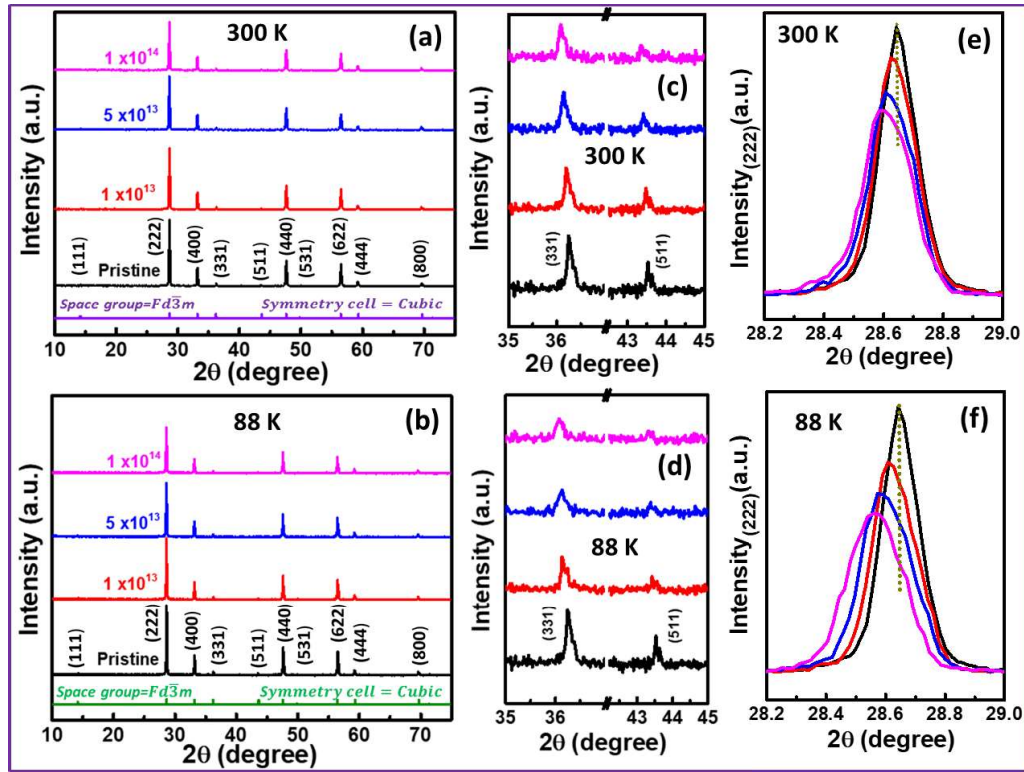


**Figure. 6** GIXRD patterns of  $\text{La}_2\text{Zr}_2\text{O}_7$  (a, b); enlarged view of (331), and (511) reflections and (c-d) magnified of (222) reflection.

HR-TEM photographs of the pristine  $\text{La}_2\text{Zr}_2\text{O}_7$  sample confirmed the well-arranged atomic ordering of pristine  $\text{La}_2\text{Zr}_2\text{O}_7$  samples.  $\text{La}_2\text{Zr}_2\text{O}_7$  sample irradiated at RT reveals the signature of deterioration of atomic ordering while  $\text{La}_2\text{Zr}_2\text{O}_7$  sample irradiated at low temperature affirmed the dilapidation of atomic ordering. Here, we would like to emphasize that the deterioration of atomic ordering of  $\text{La}_2\text{Zr}_2\text{O}_7$  samples is more significantly at low temperature than RT due to the immobile nature of defects.

Moreover, the engineering of disordering/ordering in cation and anion sub-lattices is particularly important in developing high-performance materials for advanced nuclear energy and high-temperature electrolytes systems. Therefore, to evaluate the ordering/disordering of  $\text{La}_2\text{Zr}_2\text{O}_7$  samples upon irradiation of low-energy ions ( $500 \text{ KeV Kr}^{2+}$ ), the GIXRD technique has been employed. Fig. 6 (c, d) exhibits the magnified view of superstructure reflections of before and after irradiated  $\text{La}_2\text{Zr}_2\text{O}_7$  samples and reveals the presence of superstructure



reflections. The presence of superstructure reflections in all samples at both the temperatures specifies the formation of the pyrochlore phase. The peaks shift towards to lower  $2\theta$  with the augmentation of fluence, which leads to lattice swelling [Fig. 6 (e, f)]. Interestingly, the peak shifting is relatively higher at 88 K than 300 K.

The cation order/disorder deduced from the cationic order/disorder parameter ( $\Phi$ ), exhibits the monotonous dependence of cation disorder on the ion fluence and irradiation temperature. Similarly, the oxygen positional parameter,  $x_{48f}$ , which determines the crystal structure of pyrochlore oxides, enhances monotonically with the function of ion fluence. The value of the  $x_{48f}$  parameter at 88 K is found to be higher for similar fluence than at 300 K. The relatively higher value of the  $x_{48f}$  parameter at 88 K may be associated with the relatively more pronounced disordering/defects at 88 K. Raman spectroscopy exhibits that the intensity of the vibrational modes at both the temperature decreases with the function of fluence. At the same time, the FWHM enhances with further enhancement of fluence. The weakening and broadening of vibration modes specify the distortion in the lattice, i.e., crystal lattice became stressed upon ion irradiation.

The interesting outcome of this investigation is that the  $\text{La}_2\text{Zr}_2\text{O}_7$  samples preserved the pyrochlore structure upon irradiation of 1.00 MeV  $\text{Xe}^{4+}$  and  $\text{La}_2\text{Zr}_2\text{O}_7$  samples irradiated with 500 keV  $\text{Kr}^{2+}$  ions demonstrate that the ion irradiation induced the cation and anion disordering in the system.

### **1.3.3 Radiation tolerance of $\text{Gd}_2\text{Zr}_2\text{O}_7$ upon irradiation swift heavy ion irradiation: a suitable matrix for immobilization of nuclear waste**

Materials used for effective management of (involving their safe discharge and storage) radioactive wastes should be stable in radioactive environments. Therefore, the development of radiation-resistant compounds for the effective management of radioactive wastes is of utmost importance.  $\text{Gd}_2\text{Zr}_2\text{O}_7$  samples with different structural defects were irradiated 100 MeV  $\text{I}^{7+}$  ions at the fluence of  $1.0 \times 10^{14}$  ions/cm<sup>2</sup> and explored the role of structural ordering/defects on radiation tolerance. The XRD and Raman spectroscopy analysis of pristine  $\text{Gd}_2\text{Zr}_2\text{O}_7$  samples exhibits that the  $\text{Gd}_2\text{Zr}_2\text{O}_7$  samples sintered at different temperatures possess different degrees of structural order/disordering. Further, the XRD and Raman spectroscopy studies of post irradiated  $\text{Gd}_2\text{Zr}_2\text{O}_7$  samples demonstrated that the  $\text{Gd}_2\text{Zr}_2\text{O}_7$  sample (sintered at 1500°C) with some extant of pyrochlore ordering possesses better radiation tolerance than the corresponding  $\text{Gd}_2\text{Zr}_2\text{O}_7$  sample (sintered at 1400°C).

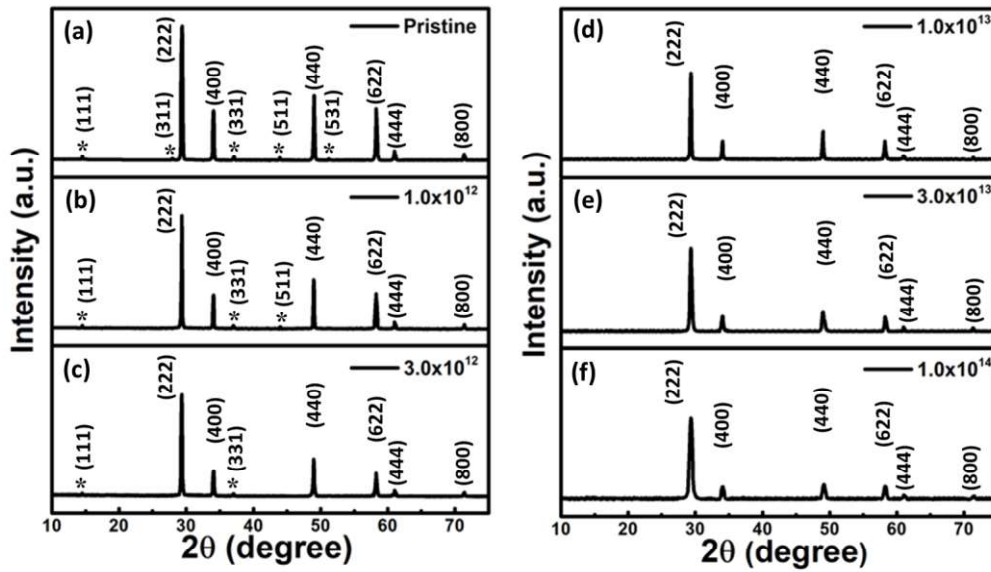


**Figure 7** XRD patterns of  $\text{Gd}_2\text{Zr}_2\text{O}_7$  sample before and after irradiation with 100 MeV  $\text{I}^{7+}$  ions as a function of ion fluence.

Further, we investigated the order-disorder (O-D) transformation in  $\text{Gd}_2\text{Zr}_2\text{O}_7$  with the augmentation of ion fluence. To explore the radiation tolerance of the GZO sample for applications in hostile environments, the GZO samples were irradiated with the 100 MeV  $\text{I}^{7+}$  ions at the fluence of  $1.0 \times 10^{12}$ ,  $3.0 \times 10^{12}$ ,  $1.0 \times 10^{13}$ ,  $3.0 \times 10^{13}$ ,  $1.0 \times 10^{14}$  ions/cm<sup>2</sup>. Fig. 7 exhibits that the diffraction peaks slightly decrease with the increase of ion fluence, and peaks width also seem to be relatively broader upon irradiation of 100 MeV iodine ions with enhanced ion fluence. The  $\text{Gd}_2\text{Zr}_2\text{O}_7$  samples demonstrate order-disorder, i.e., pyrochlore to fluorite phase transformation at the ion fluence of  $1.0 \times 10^{13}$  ions/cm<sup>2</sup>, and no signal of amorphization was perceived in the  $\text{Gd}_2\text{Zr}_2\text{O}_7$  system even at the highest ion fluence of  $1.0 \times 10^{14}$  ions/cm<sup>2</sup> which established the capabilities of GZO for possible applications in hostile environments such as immobilization of high-level radioactive waste nuclides.

## 1.4 Conclusions

A brief review of nuclear wastes generated during the operation of the nuclear power plant, types of different crystalline ceramics for immobilization of radioactive wastes, classification of pyrochlore oxides, zirconate pyrochlores, and use of pyrochlore oxides particularly zirconate pyrochlores in different technological applications are discussed.

As discussed in the introduction section, there are a lot of real and practical challenges for the safe and effective management of radioactive wastes which were difficult to overcome. However, progressive and innovative research work has presented step-by-step improvement in alteration of essential chemical and physical properties of pyrochlore oxides specially



zirconate pyrochlores as reported by the scientific community. However, the biggest challenge of designing and fabrication of complex pyrochlore oxides with the engineering of crystal structures from pyrochlore to defect fluorite is still open.

In this dissertation, we present a comprehensive approach for alteration of structural modifications of  $\text{La}_2\text{Zr}_2\text{O}_7$  and  $\text{Gd}_2\text{Zr}_2\text{O}_7$  upon annealing temperature and ion irradiation for possible application in hostile environments and other several emerging applications for societal development.

A series of zirconate pyrochlore oxides, i.e.,  $\text{La}_2\text{Zr}_2\text{O}_7$  and  $\text{Gd}_2\text{Zr}_2\text{O}_7$  samples were prepared *via* a standard solid-state method, and the impact of extremal parameters, i.e., annealing temperature, irradiation temperature, ion energy, and ion fluence on the structural modification were explored. To investigate the impact of annealing temperature and time, the  $\text{La}_2\text{Zr}_2\text{O}_7$  samples were annealed at different temperatures and times. Further, to compute the impact of irradiation temperature and ion fluence on the structural modifications of  $\text{La}_2\text{Zr}_2\text{O}_7$  samples were irradiated with 1.00 MeV  $\text{Xe}^{4+}$  and 500 keV  $\text{Kr}^{2+}$  ions. Further, the radiation tolerance of  $\text{Gd}_2\text{Zr}_2\text{O}_7$  samples with the function of different degrees of structural ordering/disordering and ion fluence upon irradiation of swift heavy ion irradiation (100 MeV,  $\text{I}^{7+}$  ions) were explored. To evaluate the annealing/sintering temperature and ion irradiation induced structural modifications the different complementary analytical characterization techniques such as XRD, GIXRD, FE-SEM, Raman spectroscopy, and HR-TEM were employed.

Structural and microstructural properties of  $\text{La}_2\text{Zr}_2\text{O}_7$  samples transformed with the augmentation of the annealing temperature and extended time duration. The XRD analysis demonstrates the enhancement in the crystallinity of the  $\text{La}_2\text{Zr}_2\text{O}_7$  samples with enrichment of annealing temperature and extended time duration. The Rietveld refinement of the  $\text{La}_2\text{Zr}_2\text{O}_7$  samples confirmed the formation of cubic structure pyrochlore phase. The qualitative evaluation of variable oxygen parameter ' $x_{48f}$ ' and cation ordering revealed the enrichment of the pyrochlore phase structure. FE-SEM results strengthen the XRD studies and established grain growth evolution of  $\text{La}_2\text{Zr}_2\text{O}_7$  samples. The grain growth component revealed that the curvature-driven migration/diffusion of grain boundaries occurred at elevated temperatures for a prolonged duration. An outcome of the investigation divulges that the preselected and destined parameters were found to be capable of tailoring the microstructure and structural ordering that enchant the research community because having tremendous applications in diverse fields.

La<sub>2</sub>Zr<sub>2</sub>O<sub>7</sub> samples irradiated in a well-controlled environment using 1.0 MeV Xe<sup>4+</sup> ions with the function of ion fluence at two different temperatures (88 K and 300 K) demonstrate the splendid structural response. The microstructural study of the un-irradiated La<sub>2</sub>Zr<sub>2</sub>O<sub>7</sub> sample exhibits that the grains and grain boundaries are evidently noticeable. The GIXRD studies exhibit the deterioration of the crystallinity of La<sub>2</sub>Zr<sub>2</sub>O<sub>7</sub> samples. The deterioration of the crystallinity enhanced monotonically with augmentation of fluence at both the temperatures. Rietveld refinement indicates that the lattice parameters of La<sub>2</sub>Zr<sub>2</sub>O<sub>7</sub> samples enhanced with the augmentation of ion fluence. Raman spectroscopy analysis suggests the concurrently weakening and broadening of the vibrational modes of La<sub>2</sub>Zr<sub>2</sub>O<sub>7</sub> samples upon irradiation and are relatively higher at ~88 K. Both, GIXRD and Raman spectroscopy indicated that the damage is more pronounced at ~ 88 K with the increment of ion fluence. The HR-TEM micrographs of La<sub>2</sub>Zr<sub>2</sub>O<sub>7</sub> samples confirmed that the deterioration of atomic ordering is more pronounced at ~88 K than 300 K.

The influence of low-energy ion irradiation (500 keV, Kr<sup>2+</sup>) on the structural response of La<sub>2</sub>Zr<sub>2</sub>O<sub>7</sub> samples was investigated with the function of irradiation temperature (88 K and 300 K) and ion fluence. The before and after irradiation of La<sub>2</sub>Zr<sub>2</sub>O<sub>7</sub> samples were studied using GIXRD and Raman spectroscopy techniques. The continuous weakening and broadening of LZO reflections with the enhancement of fluence shows the induced structural disordering at 88 K and 300 K upon irradiation and are relatively higher at a lower temperature (88 K). The lattice strain and cell volume expansion depend on the irradiation temperature and fluence; are significantly more pronounced at 88 K than 300 K. Disorder of cation and anion enhanced as a function of fluence and it is relatively higher at 88 K. Raman spectroscopy revealed the augmentation of disorder in La<sub>2</sub>Zr<sub>2</sub>O<sub>7</sub> samples with the enrichment of fluence. Further, Raman spectroscopy analysis confirmed the higher disorder/distortion in the system at 88 K. Both, the XRD and Raman spectroscopy confirmed more pronounced structural modification (defects/disordering) in La<sub>2</sub>Zr<sub>2</sub>O<sub>7</sub> samples at 88 K in comparison of 300 K due to the immobile nature of ion irradiation-induced disorder/defects.

The impact of structural ordering/disordering on the radiation tolerance of Gd<sub>2</sub>Zr<sub>2</sub>O<sub>7</sub> samples sintered at 1500°C (GZO15) and 1400°C (GZO14) has been investigated using XRD, FE-SEM, and Raman spectroscopy. Peak fitting profile analysis and Rietveld refinement of GZO14 and GZO15 samples demonstrate that both samples possess some different degrees of pyrochlore super-structural ordering. Raman spectroscopy studies also confirm the existence of the

pyrochlore phase in both GZO samples and strengthen the Rietveld analysis. The different degrees of pyrochlore phase GZO14 and GZO15 samples were irradiated using 100 MeV  $I^{7+}$  ions at the fluence of  $1.0 \times 10^{14}$  ions/cm<sup>2</sup>. Raman studies illustrate the presence of weak pyrochlore phase ordering while XRD analysis exhibited pyrochlore to fluorite phase transition upon irradiation. Both, the XRD and Raman spectroscopy studies exhibited that the GZO15 sample displays better radiation tolerance than the GZO14 sample. The better radiation tolerance of the GZO15 sample seems associated with some extent of the ordered pyrochlore phase. The results reported here are appreciable as they may pave a path for the fabrication of complex oxide materials with different degrees of ordering/disordering for better radiation tolerance. Assessment of radiation resistance of  $Gd_2Zr_2O_7$  samples establishes the feasibility of it for the possible applications in hostile environments such as radiation tolerant hosts for safe and effective management of radioactive nuclear wastes and surplus actinides.

Further,  $Gd_2Zr_2O_7$  samples were irradiated using 100 MeV  $I^{7+}$  ions and the impact of ion fluence on the structural modifications for possible use in nuclear applications was explored. XRD and Raman spectroscopy were employed to examine the radiation-induced structural modifications (O-D transformation). The Rietveld refinement of the pristine  $Gd_2Zr_2O_7$  samples exhibited the ordered pyrochlore structure. XRD analysis confirmed the irradiation induced structural modifications, i.e., pyrochlore to defect fluorite phase transition in  $Gd_2Zr_2O_7$  samples, and found to be ion fluence dependent. Specifically, the  $Gd_2Zr_2O_7$  samples irradiated for initial fluences ( $1.0 \times 10^{12}$  ions/cm<sup>2</sup> and  $3.0 \times 10^{12}$  ions/cm<sup>2</sup>) present the least degree of phase fraction. The Raman spectroscopy analysis also confirms the order-disorder in  $Gd_2Zr_2O_7$  samples. The degree of the disorder is enhanced as a function of ion fluence and disregards the appearance of amorphization. The pyrochlore to defect fluorite phase transformation without any signature of amorphization, even for the highest fluence, establishes the potentiality of GZO samples for utilization in nuclear applications as radioactive waste forms.

## References

- [1] M.R. Greenberg, Nuclear waste management, nuclear power, and energy choices, 2012. <https://doi.org/10.1007/978>.
- [2] Hyatt, Ojovan, Special Issue: Materials for Nuclear Waste Immobilization, Materials (Basel). 12 (2019) 3611. <https://doi.org/10.3390/ma12213611>.
- [3] M.I. Ojovan, W.E. Lee, S.N. Kalmykov, Nuclear Waste Types and Sources, in: An Introd. to Nucl. Waste Immobil., Elsevier, 2019: pp. 119–143. <https://doi.org/10.1016/B978-0-08-102702-8.00010-8>.
- [4] M.I. Ojovan, W.E. Lee, W. Lee, An Introduction to Nuclear Waste Immobilisation, Elsevier, 2005. <https://doi.org/10.1016/B978-0-08-044462-8.X5000-5>.
- [5] C.M. Jantzen, Historical development of glass and ceramic waste forms for high level radioactive wastes, in: Handb. Adv. Radioact. Waste Cond. Technol., Elsevier, 2011: pp. 159–172. <https://doi.org/10.1533/9780857090959.1.159>.
- [6] W.E. Lee, M.I. Ojovan, M.C. Stennett, N.C. Hyatt, Immobilisation of radioactive waste in glasses, glass composite materials and ceramics, Adv. Appl. Ceram. 105 (2006) 3–12. <https://doi.org/10.1179/174367606X81669>.
- [7] A.I. Orlova, M.I. Ojovan, Ceramic Mineral Waste-Forms for Nuclear Waste Immobilization, Materials (Basel). 12 (2019) 2638. <https://doi.org/10.3390/ma12162638>.
- [8] S. Zinatloo-Ajabshir, M. Salavati-Niasari, A. Sobhani, Z. Zinatloo-Ajabshir, Rare earth zirconate nanostructures: Recent development on preparation and photocatalytic applications, J. Alloys Compd. 767 (2018) 1164–1185. <https://doi.org/10.1016/j.jallcom.2018.07.198>.
- [9] A. Panghal, P.K. Kulriya, Y. Kumar, F. Singh, N.L. Singh, Investigations of atomic disorder and grain growth kinetics in polycrystalline La<sub>2</sub>Zr<sub>2</sub>O<sub>7</sub>, Appl. Phys. A. 125 (2019) 428. <https://doi.org/10.1007/s00339-019-2720-8>.
- [10] K. Liu, K. Zhang, T. Deng, B. Luo, H. Zhang, Heavy-ion irradiation effects of Gd<sub>2</sub>Zr<sub>2</sub>O<sub>7</sub> nanocrystalline ceramics as nuclear waste immobilization matrix, J. Nucl. Mater. 538 (2020) 152236. <https://doi.org/10.1016/j.jnucmat.2020.152236>.
- [11] G. Ou, W. Liu, L. Yao, H. Wu, W. Pan, High conductivity of La<sub>2</sub>Zr<sub>2</sub>O<sub>7</sub> nanofibers by phase control, J. Mater. Chem. A. 2 (2014) 1855–1861. <https://doi.org/10.1039/c3ta13465b>.
- [12] C.G. Liu, Y.H. Li, Y.D. Li, L.Y. Dong, J. Wen, D.Y. Yang, Q.L. Wei, P. Yang, First

- principle calculation of helium in  $\text{La}_2\text{Zr}_2\text{O}_7$ : Effects on structural, electronic properties and radiation tolerance, *J. Nucl. Mater.* 500 (2018) 72–80. <https://doi.org/10.1016/j.jnucmat.2017.12.024>.
- [13] N.. Kulkarni, S. Sampath, V. Venugopal, Preparation and characterisation of Pu-pyrochlore:  $[\text{La}_{1-x}\text{Pu}_x]_2\text{Zr}_2\text{O}_7$  ( $x=0-1$ ), *J. Nucl. Mater.* 281 (2000) 248–250. [https://doi.org/10.1016/S0022-3115\(00\)00336-6](https://doi.org/10.1016/S0022-3115(00)00336-6).
- [14] J. Lian, X.T. Zu, K.V.G. Kutty, J. Chen, L.M. Wang, R.C. Ewing, R.C. Ewing, Ion-irradiation-induced amorphization of  $\text{La}_2\text{Zr}_2\text{O}_7$  pyrochlore, *Phys. Rev. B - Condens. Matter Mater. Phys.* 66 (2002) 541081–541085. <https://doi.org/10.1103/PhysRevB.66.054108>.
- [15] M. Lang, F.X. Zhang, R.C. Ewing, J. Lian, C. Trautmann, Z. Wang, Structural modifications of  $\text{Gd}_2\text{Zr}_{2-x}\text{Ti}_x\text{O}_7$  pyrochlore induced by swift heavy ions: Disorder and amorphization, *J. Mater. Res.* 24 (2009) 1322–1334. <https://doi.org/10.1557/jmr.2009.0151>.
- [16] J. Lian, J. Chen, M. Wang, R.C. Ewing, J.M. Farmer, L.A. Boatner, B. Helean, Radiation-Induced amorphization of rare-Earth titanate pyrochlores, *Phys. Rev. B - Condens. Matter Mater. Phys.* 68 (2003) 1–9. <https://doi.org/10.1103/PhysRevB.68.134107>.
- [17] F.X. Zhang, M. Lang, R.C. Ewing, Atomic disorder in  $\text{Gd}_2\text{Zr}_2\text{O}_7$  pyrochlore, *Appl. Phys. Lett.* 106 (2015) 191902. <https://doi.org/10.1063/1.4921268>.
- [18] L. Kong, I. Karatchevtseva, D.J. Gregg, M.G. Blackford, R. Holmes, G. Triani,  $\text{Gd}_2\text{Zr}_2\text{O}_7$  and  $\text{Nd}_2\text{Zr}_2\text{O}_7$  pyrochlore prepared by aqueous chemical synthesis, *J. Eur. Ceram. Soc.* 33 (2013) 3273–3285. <https://doi.org/10.1016/j.jeurceramsoc.2013.05.011>.
- [19] M.K. Patel, V. Vijayakumar, S. Kailas, D.K. Avasthi, J.C. Pivin, A.K. Tyagi, Structural modifications in pyrochlores caused by ions in the electronic stopping regime, *J. Nucl. Mater.* 380 (2008) 93–98. <https://doi.org/10.1016/j.jnucmat.2008.07.007>.
- [20] M.K. Patel, V. Vijayakumar, D.K. Avasthi, S. Kailas, J.C. Pivin, V. Grover, B.P. Mandal, A.K. Tyagi, Effect of swift heavy ion irradiation in pyrochlores, *Nucl. Instruments Methods Phys. Res. Sect. B Beam Interact. with Mater. Atoms.* 266 (2008) 2898–2901. <https://doi.org/10.1016/j.nimb.2008.03.135>.
- [21] G. Sattonnay, S. Moll, L. Thomé, C. Legros, M. Herbst-Ghysel, F. Garrido, J.M. Costantini, C. Trautmann, Heavy-ion irradiation of pyrochlore oxides: Comparison between low and high energy regimes, *Nucl. Instruments Methods Phys. Res. Sect. B Beam Interact. with Mater. Atoms.* 266 (2008) 3043–3047.

<https://doi.org/10.1016/j.nimb.2008.03.161>.

- [22] G. Sattonnay, S. Moll, L. Thomé, C. Decorse, C. Legros, P. Simon, J. Jagielski, I. Jozwik, I. Monnet, Phase transformations induced by high electronic excitation in ion-irradiated  $\text{Gd}_2(\text{Zr}_x\text{Ti}_{1-x})_2\text{O}_7$  pyrochlores, *J. Appl. Phys.* 108 (2010) 103512. <https://doi.org/10.1063/1.3503452>.
- [23] X. Shu, L. Fan, Y. Xie, W. Zhu, S. Pan, Y. Ding, F. Chi, Y. Wu, X. Lu, Alpha-particle irradiation effects on uranium-bearing  $\text{Gd}_2\text{Zr}_2\text{O}_7$  ceramics for nuclear waste forms, *J. Eur. Ceram. Soc.* 37 (2017) 779–785. <https://doi.org/10.1016/j.jeurceramsoc.2016.09.034>.
- [24] S. Liu, T. Yang, J. Zhang, Z. Yan, Y. Lu, D. Han, C. Wang, Y. Fang, Y. Wang, Thermal effects in ion irradiated  $\text{Ti}_2\text{AlC}$  and  $\text{Ti}_3\text{SiC}_2$ , *Nucl. Instruments Methods Phys. Res. Sect. B Beam Interact. with Mater. Atoms.* 435 (2018) 50–55. <https://doi.org/10.1016/j.nimb.2017.10.006>.

## *List of Publications*

### **Peer-Reviewed Journal Publication**

1. **Asha Panghal**, Yogendra Kumar, P.K. Kulriya, P. M. Shirage, N. L. Singh “Atomic order-disorder engineering in the  $\text{La}_2\text{Zr}_2\text{O}_7$  pyrochlore under low energy ion irradiation” *Ceramics International*, 47,(14), 2021, 20248-20259, <https://doi.org/10.1016/j.ceramint.2021.04.032> **(I.F.-4.527)**.
2. **Asha Panghal**, Yogendra Kumar, P. K. Kulriya, N. L. Singh “Structural assessment and irradiation response of  $\text{La}_2\text{Zr}_2\text{O}_7$  pyrochlore: Impact of irradiation temperature and ion fluence” *Journal of Alloys and Compounds*, 862 (2021)158556, <https://doi.org/10.1016/j.jallcom.2020.158556> **(I.F.-5.316)**.
3. **Asha Panghal**, P. K. Kulriya, Yogendra Kumar, Fouran Singh, N. L. Singh “Investigations of atomic disorder and grain growth kinetics in polycrystalline  $\text{La}_2\text{Zr}_2\text{O}_7$ ” *Applied Physics A* (2019) 125:428, <https://doi.org/10.1007/s00339-019-2720-8> **(I.F.-2.584)**.
4. **Asha Panghal**, Yogendra Kumar, N. L. Singh “Investigation of structural modifications of  $\text{Gd}_2\text{Zr}_2\text{O}_7$  pyrochlore induced by swift heavy ions for nuclear waste immobilization (communicated in a peer-reviewed journal)
5. **Asha Panghal**, Yogendra Kumar, N. L. Singh “Role of structural ordering on the radiation response of  $\text{Gd}_2\text{Zr}_2\text{O}_7$  pyrochlore” (communicated in a peer-reviewed journal)

### **List of International and National Conferences/Schools/Workshops:**

#### **(a) International:**

1. **Asha Panghal**, N. L. Singh, School on Accelerator Science and Technology, 16-27<sup>th</sup> May 2016, Inter-University Accelerator Centre, New Delhi, India.
2. **Asha Panghal**, N. L. Singh, School on characterizations of materials, 04-09<sup>th</sup> September 2017, Inter-University Accelerator Centre, New Delhi, India.
3. **Asha Panghal** and N. L. Singh, International Conference on High Energy Radiation and Applications, 10-13<sup>th</sup> October 2017, The M. S. University of Baroda, Vadodara, Gujarat, India
4. **Asha Panghal**, N. L. Singh, Joint ICTP-IAEA Workshop on Fundamentals of Vitrification and Vitreous Materials for Nuclear Waste Immobilization, 06-10<sup>th</sup> November 2017, International Centre for Theoretical Physics, Trieste, Italy **(Oral presentation)**.

5. **Asha Panghal**, N. L. Singh, Joint ICTP-IAEA International School on Nuclear Waste Actinide Immobilization” 10-14<sup>th</sup> September **2018**, International Centre for Theoretical Physics, UNESCO, **Italy (Oral presentation)**.
6. **Asha Panghal** and N. L. Singh, 5th International Conference on “Ion beams in materials engineering and characterization” (**IBMEC**) 9-12<sup>th</sup> October **2018**, IUAC, New Delhi, India (**Best Poster Award\_1st prize**)
7. **Asha Panghal** and N. L. Singh, Indo-French conference on “Radiation damage in Nuclear Materials” 18-20<sup>th</sup> February **2019**, held at Amity University Noida and IUAC New Delhi, India.
8. **Asha Panghal**, N. L. Singh, Joint ICTP-IAEA International School on Radioactive Waste Cementation, 16th Oct-25<sup>th</sup> Nov **2020**, International Centre for Theoretical Physics, **Trieste, Italy**. (Virtual School\_Oral presentation).
9. **Asha Panghal**, N. L. Singh, International conference (online) on Ion Beams in Materials Engineering and Characterization (**IBMEC-2020**), 8-11<sup>th</sup>, December **2020**, held at IUAC Delhi, India (Online mode).

**(b) National:**

1. **Asha Panghal** and N. L. Singh, National Conference on Recent Trends in Materials Science, 24-25<sup>th</sup> March **2018**, held at The M. S. University of Baroda, Gujarat, India.
2. **Asha Panghal** and N. L. Singh, National conference on Nanoscience and Technologies in Digital India (NANOTCON), 27-28<sup>th</sup> April **2018**, Shobhit Deemed University, Meerut, India.
3. **Asha Panghal**, Y. Kumar, and N. L. Singh, National Conference on Recent Trends in Material Science and Technology, 7-9<sup>th</sup> December **2020**, Indian Institute of Space Science and Technology, Kerala, India.